

Single-Particle Approach to Self-Consistent Monte Carlo Device Simulation

Fabian M. BUFLER^{†a)}, Christoph ZECHNER^{††}, Andreas SCHENK[†],
and Wolfgang FICHTNER[†], *Nonmembers*

SUMMARY The validity and capability of an iterative coupling scheme between single-particle frozen-field Monte Carlo simulations and nonlinear Poisson solutions for achieving self-consistency is investigated. For this purpose, a realistic $0.1\ \mu\text{m}$ lightly-doped-drain (LDD) n-MOSFET with a maximum doping level of about $2.5 \times 10^{20}\ \text{cm}^{-3}$ is simulated. It is found that taking the drift-diffusion (DD) or the hydrodynamic (HD) model as initial simulation leads to the same Monte Carlo result for the drain current. This shows that different electron densities taken either from a DD or a HD simulation in the bulk region, which is never visited by Monte Carlo electrons, have a negligible influence on the solution of the Poisson equation. For the device investigated about ten iterations are necessary to reach the stationary state after which gathering of cumulative averages can begin. Together with the absence of stability problems at high doping levels this makes the self-consistent single-particle approach (SPARTA) a robust and efficient method for the simulation of nanoscale MOSFETs where quasi-ballistic transport is crucial for the on-current.

key words: ballistic transport, Monte Carlo simulation, nanoscale MOSFETs, nonlinear Poisson equation, self-consistency

1. Introduction

As scaling of silicon microelectronics has now reached the $0.1\ \mu\text{m}$ regime, the on-current I_{on} is increasingly influenced by quasi-ballistic transport which is not accurately taken into account by classical device simulation based on the drift-diffusion or the hydrodynamic model [1], [2]. In contrast, this effect can be adequately investigated by self-consistent full-band Monte Carlo simulation [3], [4] and this approach has been often adopted in recent works for studying the performance of nanoscale MOSFETs [1], [5]–[9]. However, in these works the ensemble Monte Carlo technique was employed which requires very small time steps on a femtosecond scale in order to avoid stability problems [10]. This has limited the practical applicability to simplified device structures with a maximum doping level considerably or even far below $1 \times 10^{20}\ \text{cm}^{-3}$. The stability problem does not exist in an alternative self-consistency scheme

where Monte Carlo solutions of the Boltzmann equation are iteratively coupled with the nonlinear Poisson equation until convergence is achieved [11]. In the present work we adopt the latter approach by coupling single-particle frozen-field Monte Carlo simulations [12] with solutions of the nonlinear Poisson equation where the electron density in the low-density bulk regions, which are never visited by the single particles, is taken from the initial classical simulation. It is, on the one hand, the aim of this paper to assess the validity of this approach by investigating whether there is a sensitivity to the type of the initial classical simulation (DD or HD) or to the length of the time interval after which the Poisson equation is solved because these variations involve different bulk densities. On the other hand, the capability of this method for treating realistic devices is demonstrated and illustrated by the simulation of an $0.1\ \mu\text{m}$ LDD n-MOSFET structure which is obtained from process simulation [13] according to a realistic process flow.

2. Monte Carlo Model and Device Structure

The full band structure is obtained from nonlocal empirical pseudopotential calculations including spin-orbit interaction and the energies of four conduction bands are stored on an equidistant mesh with a spacing of $1/96 \times 2\pi/a$ with a denoting the lattice constant. The scattering mechanisms include phonon scattering, impurity scattering, impact ionization and surface roughness scattering. The phonon system consists of three f -type and three g -type intervalley processes with the same values for the coupling constants as reported by Jacoboni and Reggiani [14] and acoustic intravalley scattering. Impurity scattering is taken into account via a calibrated Ridley model [12] where a doping-dependent prefactor of the rate is adjusted such that the measured doping dependence of the ohmic mobility [15] is reproduced. The present impact ionization scattering rate is taken from Ref. [16]. The semi-empirical surface roughness scattering model involves a combination of diffusive and specular scattering where the percentage of diffusive scattering is 15%. Details of the propagation algorithm are reported in Refs. [12], [17].

The bulk mobility model of the initial classical device simulations corresponds to the bulk Monte Carlo

Manuscript received September 4, 2002.

Manuscript revised October 18, 2002.

[†]The authors are with the Institut für Integrierte Systeme, ETH Zürich, Gloriastrasse 35, CH-8092 Zürich, Switzerland.

^{††}The author is with ISE Integrated Systems Engineering AG, Balgriststrasse 102, CH-8008 Zürich, Switzerland.

a) E-mail: bufler@iis.ee.ethz.ch

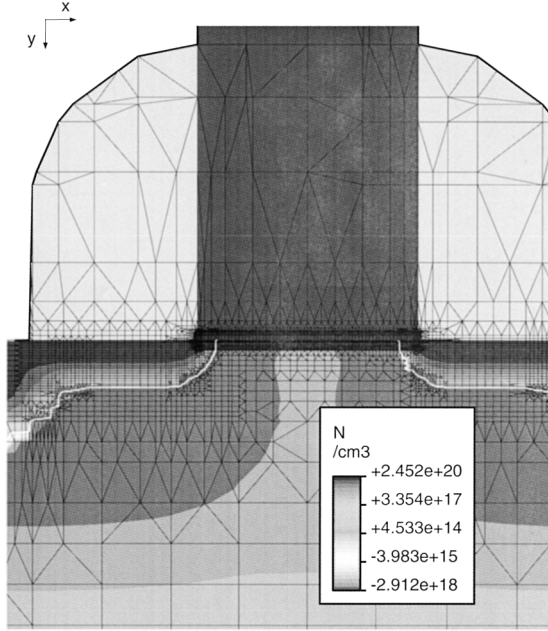


Fig. 1 Simulated n-MOSFET with $L_{\text{ch}} = 90$ nm, $L_{\text{eff}} = 75$ nm and $t_{\text{ox}} = 2.2$ nm. The white lines indicate the pn junctions.

result which entails in particular an energy relaxation time of $\tau_w = 0.3$ ps for the hydrodynamic model. The model of Darwish [18] for surface mobility reduction is adopted and bandgap narrowing, equally attributed to the valence and the conduction band edge, is modeled according to Slotboom [19]. Boltzmann statistics is used as in the Monte Carlo simulation. Finally, the above surface mobility model is adjusted in order to reproduce the Monte Carlo result for the drain current in the linear regime for the simulated $0.1 \mu\text{m}$ LDD n-MOSFET shown in Fig. 1. The device structure in Fig. 1 is obtained from process simulation [13] and features a channel length of $L_{\text{ch}} = 90$ nm, an effective gate length of $L_{\text{eff}} = 75$ nm, an oxide thickness of $t_{\text{ox}} = 2.2$ nm and a maximum doping level of about $2.5 \times 10^{20} \text{ cm}^{-3}$. The channel direction, i.e. the x axis in Fig. 1, corresponds to the crystallographic (110) direction as is usual in standard complementary metal-oxide-semiconductor (CMOS) technology.

3. Self-Consistency Scheme

When the first single-particle frozen-field Monte Carlo simulation based on the electrostatic potential ψ resulting from the initial classical simulation is completed, an estimate for the electron density n_{MC} has been obtained. It enters the Poisson equation

$$-\nabla \cdot (\epsilon \nabla \psi) = -e (n_{\text{MC}} - p + N_{\text{A}}^- - N_{\text{D}}^+) \quad (1)$$

which gives the new electric field to be used in the next Monte Carlo simulation. Here, ϵ is the dielectric constant, $e > 0$ the elementary charge, p the hole density,

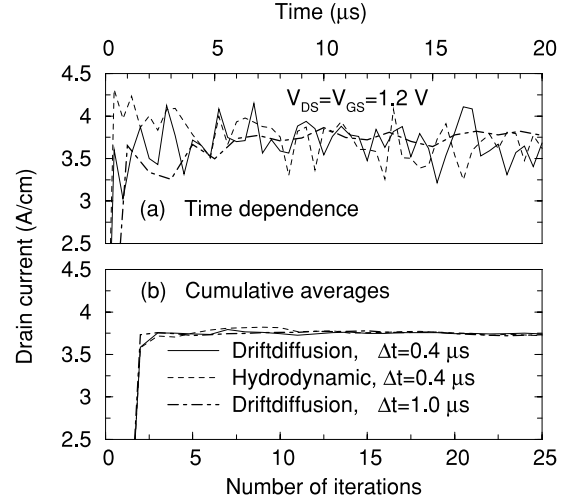


Fig. 2 (a) Drain current as a function of the time, during which single particles are simulated, and (b) cumulative averages as a function of the number of iterations taken over the values of (a) after ten iterations (i.e. after $4 \mu\text{s}$ for $\Delta t = 0.4 \mu\text{s}$ and $10 \mu\text{s}$ for $\Delta t = 1.0 \mu\text{s}$, respectively). The different curves correspond to Monte Carlo simulations based either on an initial drift-diffusion or a hydrodynamic simulation and involve different lengths Δt of the time intervals after which the nonlinear Poisson equation is solved.

N_{A}^- the acceptor concentration and N_{D}^+ the donor concentration. However, Eq. (1) which is linear in ψ gives rise to stability problems at high doping concentrations necessitating very small time steps on a femtosecond scale during ensemble Monte Carlo simulations [10], [11]. Therefore we adopt the alternative stable self-consistency scheme proposed by Venturi et al. [11]. In this scheme an electron quasi-fermi level is defined via

$$\phi_n \equiv \psi - \frac{k_B T_L}{e} \ln \left(\frac{n_{\text{MC}}}{n_{i,\text{eff}}} \right) \quad (2)$$

and likewise for holes with k_B denoting the Boltzmann constant, T_L the lattice temperature and $n_{i,\text{eff}}$ the effective intrinsic carrier concentration. Keeping the quasi-fermi level fixed and resolving Eq. (2) for n_{MC} leads to an expression for the density which depends on the potential, i.e. $n_{\text{MC}}(\psi)$. Inserting this expression into Eq. (1) makes the Poisson equation nonlinear in ψ . Then, solutions of the nonlinear Poisson equation have to be iterated with Monte Carlo solutions of the Boltzmann transport equation until convergence versus the steady-state is achieved after which gathering of cumulative averages can begin to reduce the Monte Carlo noise for the final result.

Figure 2(a) shows the evolution of the drain current as a function of the time, during which single particles are simulated, and Fig. 2(b) shows the corresponding cumulative average as a function of the number of iterations after the steady-state has been reached. In the framework of the single-particle approach without statistical enhancement, the bulk region is hardly ever visited by Monte Carlo electrons due to the small elec-

tron density in the bulk. Therefore the electron density in this region is taken from the initial classical simulation as is the hole density in the whole device. However, the electron bulk densities are significantly different between DD and HD. Also the extension of the inversion channel into the bulk, which is visited by Monte Carlo electrons, varies depending on the length Δt of the time interval after which the nonlinear Poisson equation is solved, because during a longer time interval also regions with a lower density and hence a lower probability of being visited are sampled. This raises the question how those density differences affect the solution of the Poisson equation and the resulting drain current. Therefore three different simulations are displayed in Fig. 2 based either on an initial HD or DD simulation or on different time interval lengths ($\Delta t = 0.4 \mu\text{s}$ or $\Delta t = 1.0 \mu\text{s}$) of a single frozen-field Monte Carlo simulation. It can be seen in Fig. 2(a) that the drain current begins in all three cases to fluctuate around the steady-state after roughly ten iterations, i.e. after $4 \mu\text{s}$ for $\Delta t = 0.4 \mu\text{s}$ and after $10 \mu\text{s}$ for $\Delta t = 1.0 \mu\text{s}$. Despite different shapes in the initial phase (e.g. the simulation based on an initial HD simulation features a kind of overshoot) the currents tend afterwards to fluctuate around the same value. This becomes obvious in Fig. 2(b) where the cumulative averages after ten iterations over the values in Fig. 2(a) are shown. Hence, the same results for the drain current in Fig. 2(b) suggest that the differences between the three kinds of simulation for the electron density in the bulk, where the density level is small compared to the source/drain regions and the inversion channel, are negligible for the solution of the Poisson equation. While the number of iterations necessary for reaching the steady-state seems to be the same for DD and HD, it is also clear that a time interval as small as possible is to be preferred because it reduces the simulation time for reaching the stationary state. Of course, in any case sufficient statistics for the electron density in the inversion channel must be gathered so that Δt must not be too small. In this respect, the value of $\Delta t = 0.4 \mu\text{s}$ is close to the minimum which can be safely used in the present example.

Finally, the statistical nature of the Monte Carlo simulations is illustrated in Fig. 3. There the cumulative average, i.e. the mean value

$$\bar{I} \equiv \frac{1}{n} \sum_{i=1}^n I_i \quad (3)$$

of the current values I_i with n denoting the number of iterations, can be seen for (a) the drain current and (b) the substrate current where all three simulations are based on the same initial simulation (DD) and the same time interval length ($\Delta t = 0.4 \mu\text{s}$). In Fig. 4, the corresponding relative errors

$$\Delta I \equiv 2\bar{\sigma}/\bar{I} \quad (4)$$

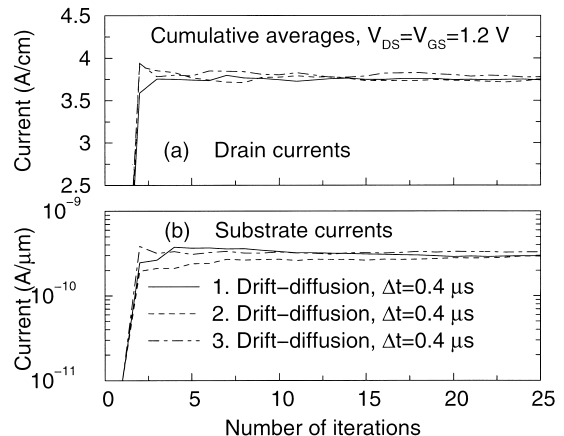


Fig. 3 Cumulative averages for (a) the drain current and (b) the substrate current as a function of the number of iterations for three simulations all based on the same initial classical device simulation and the same time interval length Δt .

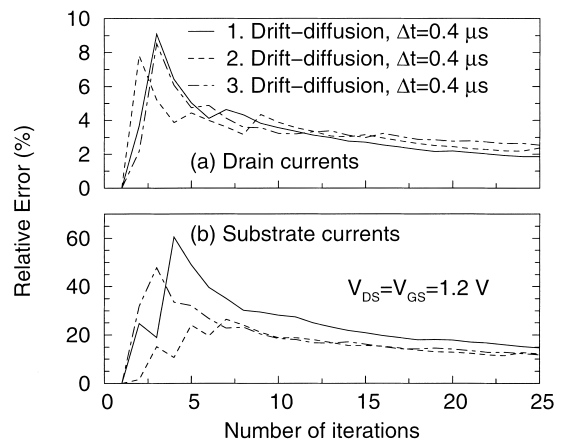


Fig. 4 Relative error corresponding to the averages in Fig. 3 for (a) the drain current and (b) the substrate current as a function of the number of iterations for three simulations all based on the same initial classical device simulation and the same time interval length Δt .

$$\bar{\sigma}^2 \equiv \frac{1}{n} \frac{1}{n-1} \sum_{i=1}^n (I_i - \bar{I})^2 \quad (5)$$

are shown with $\bar{\sigma}^2$ being the variance of the mean value. As discussed before, gathering of cumulative averages begins only after the stationary state has been reached. However, the current estimations of the subsequent iterations are not exactly stochastically independent, as it is the case for non-selfconsistent simulations [20], because two successive iterations are still coupled via the Poisson equation. As a consequence, the usual interpretation of the relative error for the confidence interval of the expectation value does not hold exactly. Nevertheless, from a practical point of view, the 'relative errors' in Fig. 4 still show the usual $1/\sqrt{n}$ behavior and can therefore be used as stopping criteria to discriminate between the different simulation times necessary at different bias points for a similar level of accuracy. The

results of one simulation after 25 iterations following steady-state as shown in Figs. 3 and 4 correspond to a CPU time of 14 h on one 667 MHz alpha processor. Note, however, that the simulation time for one bias point strongly depends on geometry and doping profiles of the device under consideration.

4. Device Simulation Results

In this section, the simulation results of the drift-diffusion model, the hydrodynamic model and the Monte Carlo model are compared. Figure 5 shows the output characteristics corresponding to the three transport models. Note that apart from the modification of the DD/HD surface mobility in order to reproduce the MC drain current at $V_{DS} = 50$ mV no further adjustment was performed. The agreement with the Monte Carlo results continues for the hydrodynamic simulation to higher drain voltages than for the drift-diffusion simulation, but the overestimation of the on-current is considerably stronger by HD than the underestimation by DD.

The differences of the on-current are related to the distribution of internal variables which are displayed in Figs. 6 and 7. The figures show the profiles of the internal variables along the channel, i.e. along the x axis in Fig. 1. They are computed by averaging the quantity perpendicular to the Si/SiO₂ interface with the relative electron density according to

$$v_x(x) \equiv \frac{\int v_x(x, y) n(x, y) dy}{\int n(x, y) dy} \quad (6)$$

as for the x -component of the drift velocity in Fig. 7(a) and likewise for the electron density $n(x)$ in Fig. 6(b) and the longitudinal electric field $E_x(x)$ in Fig. 7(b) or by integration of the quantity over y according to

$$n_{\text{inv}}(x) \equiv \int n(x, y) dy \quad (7)$$

as for the inversion layer density n_{inv} in Fig. 6(a), respectively. The figures show that the different on-currents are associated with a different drift velocity in the source-side of the channel which mainly determines I_{on} . The behavior in the drain-side of the channel is then determined by the continuity equation for the charge density. This requires e.g. the compensation of the low DD drift velocity, which cannot be higher than the saturation velocity, by a higher electron concentration so that the current remains constant in the channel.

5. Conclusions

The validity of the single-particle approach for self-consistent full-band Monte Carlo device simulation has been investigated. In this approach, single-particle

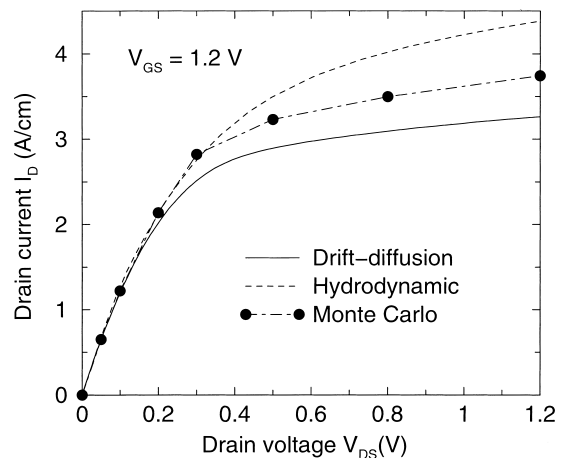


Fig. 5 Output characteristics of the 0.1 μm LDD n-MOSFET in Fig. 1 according to a drift-diffusion, a hydrodynamic and a self-consistent full-band Monte Carlo simulation.

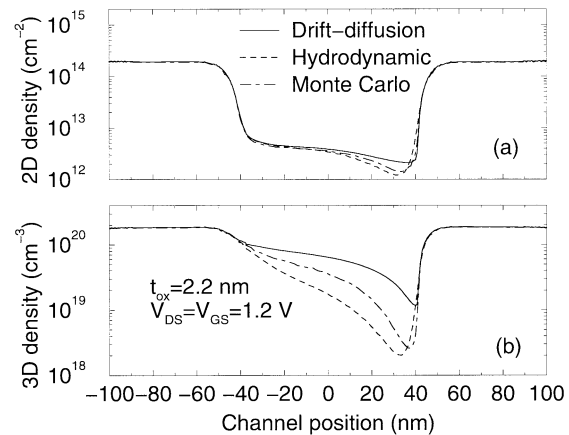


Fig. 6 Profiles along the channel of (a) the 2D inversion layer density obtained by integration of the density perpendicular to the Si/SiO₂ interface (i.e. in y -direction in Fig. 1) and (b) the mean 3D density resulting from averaging perpendicularly to the interface with the relative density.

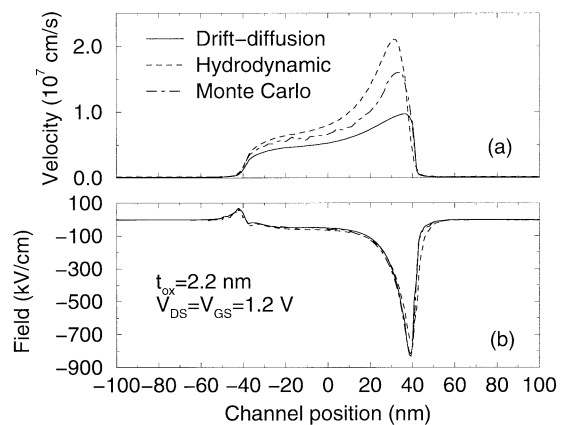


Fig. 7 Profiles along the channel of (a) the averaged electron velocity and (b) the averaged longitudinal electric field. Averaging is performed perpendicular to the Si/SiO₂ interface with the relative electron density.

frozen-field simulations are iterated with solutions of the nonlinear Poisson equation until convergence is achieved. It was found that different densities imposed for the bulk region, which is never visited by Monte Carlo electrons, have a negligible influence on the final Monte Carlo result for the drain current and can be taken e.g. either from an initial drift-diffusion or a hydrodynamic simulation. The feasibility and importance of this Monte Carlo approach was demonstrated by the simulation of a realistic $0.1\ \mu\text{m}$ n-MOSFET where the on-currents of the drift-diffusion and the hydrodynamic model strongly deviate from the Monte Carlo result. In conjunction with the stability of the nonlinear Poisson equation in high-doping regions this approach presents a viable and important tool for the consideration of quasi-ballistic transport in the sub $0.1\ \mu\text{m}$ regime.

Acknowledgement

This work was in part supported by the Kommission für Technologie und Innovation under Contract 4082.2.

References

- [1] J.D. Bude, "MOSFET modeling into the ballistic regime," Proc. SISPAD, pp.23–26, Seattle, U.S.A., Sept. 2000.
- [2] K. Banoo and M.S. Lundstrom, "Electron transport in a model Si transistor," Solid-State Electron., vol.44, pp.1689–1695, 2000.
- [3] M.V. Fischetti and S.E. Laux, "Monte Carlo analysis of electron transport in small semiconductor devices including band-structure and space-charge effects," Phys. Rev. B, vol.38, pp.9721–9745, 1988.
- [4] K. Hess, ed., Monte Carlo Device Simulation: Full Band and Beyond, Kluwer, Boston, 1991.
- [5] A. Duncan, U. Ravaioli, and J. Jakumeit, "Full-band Monte Carlo investigation of hot carrier trends in the scaling of metal-oxide-semiconductor field-effect transistors," IEEE Trans. Electron Devices, vol.45, no.4, pp.867–876, 1998.
- [6] C. Jungemann, S. Keith, M. Bartels, and B. Meinerzhagen, "Efficient full-band Monte Carlo simulation of silicon devices," IEICE Trans. Electron., vol.E82-C, no.6, pp.870–879, June 1999.
- [7] C. Jungemann and B. Meinerzhagen, "Impact of the velocity overshoot on the performance of NMOSFETs with gate lengths from 80 nm to 250 nm," Proc. ESSDERC, ed. H.E. Maes, R.P. Mertens, G. Declerck, and H. Grünbacher, vol.29, pp.236–239, Editions Frontières, Leuven, 1999.
- [8] W.J. Gross, D. Vasileska, and D.K. Ferry, "Ultrasmall MOSFETs: The importance of the full Coulomb interaction on device characteristics," IEEE Trans. Electron Devices, vol.47, no.10, pp.1831–1837, 2000.
- [9] G.F. Formicone, M. Saraniti, D.Z. Vasileska, and D.K. Ferry, "Study of a 50-nm nMOSFET by ensemble Monte Carlo simulation including a new approach to surface roughness and impurity scattering in the Si inversion layer," IEEE Trans. Electron Devices, vol.49, no.1, pp.125–132, 2002.
- [10] P.W. Rambo and J. Denavit, "Time stability of Monte Carlo device simulation," IEEE Trans. Comput.-Aided Des. Integr. Circuits Syst., vol.12, no.11, pp.1734–1741, 1993.
- [11] F. Venturi, R.K. Smith, E.C. Sangiorgi, M.R. Pinto, and B. Riccò, "A general purpose device simulator coupling poisson and Monte Carlo transport with applications to deep submicron MOSFET's," IEEE Trans. Comput.-Aided Des. Integr. Circuits Syst., vol.8, no.4, pp.360–369, 1989.
- [12] F.M. Bufler, A. Schenk, and W. Fichtner, "Efficient Monte Carlo device modeling," IEEE Trans. Electron Devices, vol.47, no.10, pp.1891–1897, 2000.
- [13] ISE Integrated Syst. Eng. AG, DIOS_{ISE} Ref. Manual, 2002.
- [14] C. Jacoboni and L. Reggiani, "The Monte Carlo method for the solution of charge transport in semiconductors with application to covalent materials," Rev. Mod. Phys., vol.55, pp.645–705, 1983.
- [15] G. Masetti, M. Severi, and S. Solmi, "Modeling of carrier mobility against carrier concentration in arsenic-, phosphorus-, and boron-doped silicon," IEEE Trans. Electron Devices, vol.30, no.7, pp.764–769, 1983.
- [16] E. Cartier, M.V. Fischetti, E.A. Eklund, and F.R. McFeely, "Impact ionization in silicon," Appl. Phys. Lett., vol.62, pp.3339–3341, 1993.
- [17] F.M. Bufler, A. Schenk, and W. Fichtner, "Proof of a simple time-step propagation scheme for Monte Carlo simulation," Mathematics and Computers in Simulation (in press).
- [18] M.A. Darwish, J.L. Lentz, M.R. Pinto, P.M. Zeitzoff, T.J. Krutsick, and H.H. Vuong, "An improved electron and hole mobility model for general purpose device simulation," IEEE Trans. Electron Devices, vol.44, no.9, pp.1529–1538, 1997.
- [19] D.B.M. Klaassen, J.W. Slotboom, and H.C. de Graaff, "Unified apparent bandgap narrowing in n- and p-type silicon," Solid-State Electron., vol.35, pp.125–129, 1992.
- [20] F.M. Bufler, A. Schenk, and W. Fichtner, "Efficient Monte Carlo device simulation with automatic error control," Proc. SISPAD, pp.27–30, Seattle, U.S.A., Sept. 2000.



Fabian M. Bufler studied physics at the TU Braunschweig and RWTH Aachen (both Germany) including an academic year at the Université de Grenoble I (France) with a scholarship of the Studienstiftung des deutschen Volkes and received the Dipl.-Phys. degree in 1992. Afterwards he joined the Institut für Theoretische Elektrotechnik, RWTH Aachen, and moved in 1995 together with the group of Prof. B. Meinerzhagen to the Institut für Theoretische Elektrotechnik und Mikroelektronik, Universität Bremen (Germany), where he received his doctor's degree in 1997. Since then he is with the Institut für Integrierte Systeme, ETH Zürich, working in the field of TCAD on Monte Carlo device modeling and transport theory.



Christoph Zechner was born in Graz, Austria, in 1972. He studied physics at the Technical University of Graz, the University of Sussex, UK, and the University of Konstanz, Germany. In 1996, he received a Dipl.-Ing. degree from the Technical University of Graz, and in 2000 a Ph.D. from the University of Konstanz for experimental work and computer simulations of silicon solar cells. In 2000, he joined ISE AG in Switzerland.

His main interest is the calibration of implantation and diffusion process simulation and the computer simulation of MOSFETs.



Andreas Schenk was born in Berlin, Germany, in 1957. He received the Diploma in physics and the Ph.D. in theoretical physics from the Humboldt University Berlin (HUB) in 1981 and 1987, respectively. In 1987 he became a research assistant at the Department of Semiconductor Theory of HUB, and 1988 he joined the R&D division of WF Berlin. From 1987 till 1991 he was working on various aspects of the physics and simulation

of optoelectronic devices, esp. infrared detector arrays, and the development and implementation of physical models for modeling infrared sensors. He is now with ETH, Zurich, Switzerland, as a senior lecturer at the Integrated Systems Laboratory. His main activities are in the development of physics-based models for simulation of submicron silicon devices. He is a member of the German Physical Society (DPG).



Wolfgang Fichtner received the Dipl.Ing. degree in physics and the Ph.D. degree in electrical engineering from the Technical University of Vienna, Austria, in 1974 and 1978, respectively. From 1975 to 1978, he was an Assistant Professor in the Department of Electrical Engineering, Technical University of Vienna. From 1979 through 1985, he worked at AT&T Bell Laboratories, Murray Hill, NJ. Since 1985 he is Professor and Head

of the Integrated Systems Laboratory at the Swiss Federal Institute of Technology (ETH). In 1993, he founded ISE Integrated Systems Engineering AG, a company in the field of technology CAD. Wolfgang Fichtner is a Fellow of the IEEE, a member of the Swiss National Academy of Engineering, and a corresponding member of the Austrian Academy of Sciences. In 2000, he received the IEEE Grove Award.